

Holographic Krylov complexity in confining gauge theories

Ali Fatemiabhari,^a Horatiu Nastase,^b Carlos Nunez and Dibakar Roychowdhury^d

^a*Institute for Theoretical and Mathematical Physics, Lomonosov Moscow State University, 119991 Moscow, Russia*

^b*Instituto de Física Teórica, UNESP-Universidade Estadual Paulista R. Dr. Bento T. Ferraz 271, Bl. II, Sao Paulo 01140-070, SP, Brazil*

^d*Department of Physics, Indian Institute of Technology Roorkee, Roorkee 247667, Uttarakhand, India*

ABSTRACT: We study holographic Krylov complexity in the Anabalón–Ross solitonic background, a top-down Type IIB solution describing a twisted-circle compactification of $\mathcal{N} = 4$ SYM that flows to a confining, gapped three-dimensional theory. Following the proposal that the time derivative of Krylov complexity is dual to the proper radial momentum of a falling bulk particle, we analyze probe geodesics in this geometry. We obtain exact analytic solutions for the radial trajectory in terms of elliptic functions, confirming and extending UV and IR asymptotic expansions. The proper momentum and resulting complexity exhibit oscillatory behaviour, which we interpret as a holographic signature of the finite Hilbert-space truncation induced by the UV cutoff together with the IR end-of-space. Our results provide a controlled top-down test of the spread-momentum correspondence and highlight qualitative differences between conformal and confining holographic dynamics.

Contents

1	Introduction and General Idea	1
2	The background of Anabalón and Ross	3
3	Geodesic motion in the Anabalón-Ross background	4
3.1	Asymptotic expansions in the SUSY case ($\mu = 0$)	6
3.2	Exact solution in the SUSY case ($\mu = 0$)	7
4	The proper momentum and complexity	9
4.1	A field theoretical approach?	11
5	Conclusions and Outlook	12
A	Elliptic Integrals	14
A.1	An explicit calculation	15
B	Exact solution for $\mu \neq 0$ and $Q \neq 0$	17

1 Introduction and General Idea

There are various notions of complexity in the available bibliography. Indeed, circuit complexity, OTOC, Path Integral optimization (tensor networks), operator growth and Krylov complexity. The latter one occupies us here. In this line there was recent progress, that we might briefly summarise as follows.

The geometric framework of [1] shows that operator growth under the Liouvillian induces a natural information geometry on the Krylov basis, where Krylov complexity corresponds to geodesic volume and Lanczos coefficients encode curvature. The work [2] generalises Krylov complexity to a family of operator-growth diagnostics with universal bounds. The momentum-Krylov correspondence proposed by [3] establishes that the boundary growth rate of Krylov complexity mirrors the radial momentum of an in-falling bulk particle across a variety of AdS black holes. The paper [4] revisits this correspondence, refining conditions under which K-complexity mirrors bulk particle dynamics and exploring possible corrections. Collectively, these works develop Krylov complexity as a geometric and potentially universal probe of chaotic evolution, preparing the ground for its holographic interpretation.

There is another line of works (that this paper does not follow upon) dealing with double-scaled SYK, JT gravity and de-Sitter. For some papers on this line see [5–8]. For recent and nicely written reviews, see [9–11]

Recent works [12] have demonstrated a sharp holographic link between the rate of spread complexity and the proper radial momentum of bulk probes, suggesting a direct bulk dual for Krylov-type measures. This was proposed in the case of conformal theories, matching nicely with a calculation in AdS, by virtue of Maldacena’s conjecture [13]. In fact, the authors of [12] proposed that the rate of spread (Krylov) complexity, maps to the proper radial momentum of a falling bulk particle in AdS-space-time.

A natural and necessary extension is to test and extend this identification and proposal to top-down backgrounds dual to confining field theories. This can be motivated as follows: confinement changes qualitatively the correlations in a system, by suppressing correlators and reducing the growth of entanglement (constraining the propagation of information) [14]. It has also been suggested that the Krylov complexity can act as an order parameter for confinement-deconfinement transitions [15]. Along these same lines it has been proposed that the entanglement entropy can act as a diagnosis of confinement [16, 17]. In parallel, a recent study for a lattice model (a modified version of the Ising model [18]) found that the onset of confinement suppresses the growth of complexity (in contrast to the conformal situation). The systems studied in [15, 18] either need of dedicated numerical analysis and/or the holographic backgrounds used are dual to systems that are not conformal in the UV. In this paper we present a holographic model, for a four dimensional CFT that flows to a confining field theory and permits to calculate exact (analytic) expressions for the complexity. This complements a companion paper [19] in which we calculated the generic evolution of holographic complexity for a four dimensional CFT, $\mathcal{N} = 4$ SYM, and an upcoming one on the holographic complexity of one- and two-dimensional quiver CFTs.

The Anabalón–Ross solitonic solution provides a top-down Type IIB background which realises a twisted S^1 compactification of $\mathcal{N} = 4$ Super Yang-Mills. This field theory flows to a gapped three dimensional theory in the IR; its exact (analytically known) metric functions and two tunable parameters (Q and μ) make this model an excellent laboratory to test holographic proposals for complexity beyond the conformal case.

Previous holographic complexity studies in confining models (in the sense of the Complexity equals Volume proposal) have observed non-trivial signatures of confinement such as a particular dependence on UV-cutoff and IR-generated scale (the analog of Λ_{QCD})—see for example [20–25]. These findings motivate the calculation of Krylov/spread complexity from a probe motion and the comparison with the Volume-proposal.

As we mentioned above, complexity calculations usually need dedicated numerical analysis. In the Anabalón–Ross background it is possible to achieve analytic control as shown in this paper.

The Anabalón–Ross geometry interpolates between large radial z coordinate AdS-behaviour and an IR smooth ‘end of space’ at finite radial coordinate z_* . Once a UV cutoff is introduced to ‘launch’ the probe into the space, this geometric truncation of the space maps to a finite effective Hilbert space for the dual state. This naturally leads to oscillatory complexity rather than unbounded growth. This is a qualitative departure from pure AdS intuition.

The two parameters characterising the model: Q associated with a Wilson line and μ corresponding with SUSY-breaking, control both the location of the end of space and

the time-scale t_e taken for the probe to arrive to the end of space z_* . Therefore these parameters provide a tunable handle to correlate geometric IR data with operator growth and complexity saturation.

Beyond testing the proposal and relations in [12], The Anabalón-Ross model allows us to confront several open questions simultaneously. For example, how Krylov coefficients or Lanczos data behave in confining flows? Whether complexity measures detect the mass gap and glueball (Λ_{QCD}) scale found in other top-down constructions. And, how SUSY or non-SUSY flows affect operator spread.

Combining the analytic geodesics and proper-momentum definition with a top-down confining geometry we can: test the universality of the spread-momentum correspondence, characterise confinement signatures in Krylov complexity, and roughly propose concrete field-theory diagnostics that should be calculable in the dual twisted compactification.

The contents of this paper are organised as follows: in Section 2 we give a brief but careful description of the Anabalón-Ross model for a twisted compactification of $\mathcal{N} = 4$ SYM that confines. To help the reader, we provide various references in which the model was analysed and extended in different ways.

In Section 3 we start the study of geodesic for the probe particle in the holographic model. For simplicity, we focus here on the SUSY case, with the parameter $\mu = 0$. We reach an ordinary differential equation of which we study the solutions in asymptotic form. This asymptotic analysis reveals the usual AdS-behaviour in the UV, but a qualitatively different result in the IR. This analysis is then confirmed by an exact analytic solution, which we write in terms of Jacobi special functions in Section 3.2. This exact solution allows us to write analytic expressions for the time to reach the end of the space, then analytic expressions for the ‘proper momentum’ and the complexity that are defined and carefully calculated in Section 4. The main observation is the oscillatory character of it (plots of analytic results clearly display this). We associate this type of behaviour with the finiteness of the dual QFT Hilbert space. In fact, in our calculation we introduced a UV-cutoff and the system has a natural IR-wall. Some analysis of these results is followed by the conclusions and future directions in Section 5. The appendices collect technical details. In particular, Appendix A carefully explains how we obtain the exact solution of Section 3 and it is warmly recommended to any reader planning to work with this material. Appendix B carefully describes the analytic solution for the geodesic in the case in which SUSY is broken (this includes as a particular case, the background of Horowitz and Myers [26]), the proper momentum and the complexity are also worked out, and compared to the ones in the SUSY case.

2 The background of Anabalón and Ross

We consider the calculation of complexity using the holographic dual to a field theory that is conformal and four dimensional at high energies. This CFT_4 spontaneously compactifies to a three-dimensional theory, confining at long distances. The background is written in [27]. The analysis of the field theory dual (a twisted-circle compactification of $\mathcal{N} = 4$ SYM) and models along similar lines (with richer dynamics) are further analysed in other

systems [20, 23–25, 28–37]. Whilst here we focus on the Anabalón-Ross model, it would be interesting to perform our calculation for the related backgrounds in [20, 23–25, 28–37]. In fact, the dynamics of these other models is richer and this could lead to interesting surprises with the complexity.

The background consists of a metric, a constant dilaton and a Ramond-Ramond five form (not quoted here). We use coordinates $[t, x_1, x_2, \phi, z, \theta, \psi, \varphi_1, \varphi_2, \varphi_3]$ to describe the metric that reads,

$$\begin{aligned} ds_{10}^2 &= \frac{l^2}{z^2} \left[-dt^2 + dx_1^2 + dx_2^2 + f(z)d\phi^2 + \frac{dz^2}{f(z)} \right] + l^2 d\tilde{\Omega}_5^2, \\ d\tilde{\Omega}_5^2 &= d\theta^2 + \sin^2 \theta d\psi^2 + \sin^2 \theta \sin^2 \psi (d\varphi_1 - A_1)^2 + \\ &\quad \sin^2 \theta \cos^2 \psi (d\varphi_2 - A_1)^2 + \cos^2 \theta (d\varphi_3 - A_1)^2. \\ A_1 &= A_\phi d\phi, \quad A_\phi = Q(z^2 - z_*^2), \quad f(z) = 1 - \mu l^2 z^4 - (Ql z)^6. \end{aligned} \tag{2.1}$$

The parameter z_* is the value of the z -coordinate for which the function $f(z_*) = 0$ (this indicates the 'end of the space', that ranges in $0 \leq z \leq z_*$). The parameter μ is chosen to be $\mu = \frac{(1-Q^6 l^6 z_*^6)}{l^2 z_*^4}$. We impose a particular periodicity for ϕ to be $L_\phi = \frac{4\pi}{f'(z_*)} = \frac{2\pi z_*}{2+(Ql z_*)^6}$. With this periodicity the subspace defined by $[z, \phi]$ becomes flat as $z \approx z_*$, avoiding a conical singularity. At the position z_* (associated with the lowest available energy in the dual QFT), the field theory is effectively three-dimensional. If the parameter $\mu = 0$ the field theory preserves four supercharges (otherwise SUSY is broken). We will be mostly concerned with the SUSY situation in what follows.

Briefly, the dynamics of the field theory proceeds as follows. At high energy (for $z \approx 0$), the field theory is conformal and SUSY. The ϕ -direction is compactified on a circle S^1 and twisted with the R-symmetry $SO(6)_R$, using a $U(1)^3$ subgroup. This preserves four supercharges if $\mu = 0$ (equivalently $z_* = \frac{1}{Ql}$). An RG-flow ensues and as we move towards the IR the KK-massive modes decouple, leaving us with a three dimensional field theory with a Chern-Simons term see [32, 38] for careful explanations. The background is dual to a confining and gapped field theory. This can be seen by the direct calculation of the Wilson-Maldacena loop, that indicates an area law—see for example [23–25].

In what follows, we perform explicitly the holographic calculation of the Krylov/spread complexity in the confining field theory described above. This calculation is different from others in the bibliography, like [12]. In fact, our calculation is top-down (done in a well-defined Type IIB background). In the UV regime we find the $SL(2)$ symmetry inside AdS_5 as in [12], but the result of the calculation is very different in the IR regime (for $z \sim z_*$). In order to perform our analysis, we study a probe particle falling in the Anabalón-Ross background of eq.(2.1).

3 Geodesic motion in the Anabalón-Ross background

As we advanced above, we consider a particle moving in the background of eq.(2.1). The geodesic is described in terms of the coordinates $[z(t), \phi(t)]$ depending on time. It is consistent to assume that all other coordinates are fixed. Working in Einstein frame (which

in this case is equivalent to string frame as the dilaton vanishes), we calculate the induced line element for this particle,

$$ds_{ind}^2 = \frac{l^2 dt^2}{z^2} \left(-1 + (f(z) + z^2 A_\phi^2) \dot{\phi}^2 + \frac{\dot{z}^2}{f(z)} \right). \quad (3.1)$$

This point particle action is

$$\mathcal{S}_P = -m \int dt \mathcal{L}_P, \quad \mathcal{L}_P = \sqrt{-\det g_{ind}} = \frac{l}{z} \sqrt{1 - z^2 M(z) \dot{\phi}^2 - \frac{\dot{z}^2}{f(z)}}. \quad (3.2)$$

We defined the function $M(z) = \frac{f(z)}{z^2} + A_\phi(z)^2$ and in what follows we set $ml = 1$.

The Lagrangian in eq.(3.2) has two conserved quantities. The first one is the angular momentum associated with translations along the ϕ -cycle,

$$L_\phi = \frac{zM(z)\dot{\phi}}{\sqrt{1 - z^2 M(z) \dot{\phi}^2 - \frac{\dot{z}^2}{f(z)}}}. \quad (3.3)$$

The second conserved quantity is the Hamiltonian (a consequence of time translation symmetry in the bulk). It reads

$$\mathcal{H} = \frac{1}{z \sqrt{1 - z^2 M(z) \dot{\phi}^2 - \frac{\dot{z}^2}{f(z)}}}. \quad (3.4)$$

For simplicity, let us focus on the situation $\dot{\phi}(t=0) = 0$. Using eq.(3.4) and $L_\phi = 0$ we obtain

$$\dot{z}(t) = \frac{1}{\mathcal{H}z} \sqrt{f(z)(\mathcal{H}^2 z^2 - 1)}. \quad (3.5)$$

Upon integrating eq.(3.5), we find

$$\int dz \frac{z}{\sqrt{-1 + \bar{\alpha}z^2 + \beta z^4 + \gamma z^6 - \zeta z^8}} = \frac{1}{\mathcal{H}}(t - t_0), \quad (3.6)$$

$$\bar{\alpha} = \mathcal{H}^2; \quad \beta = \mu l^2; \quad \gamma = Q^6 l^6 - \mu \mathcal{H}^2 l^2; \quad \zeta = Q^6 l^6 \mathcal{H}^2.$$

It can be checked that the first order equation (3.5) and its integral (3.6) do solve the Euler-Lagrange equations derived from the Lagrangian in eq.(3.2) for the case $\dot{\phi} = 0$. Consider the Hamiltonian in eq.(3.4),

$$\mathcal{H} = \frac{1}{z \sqrt{1 - \frac{\dot{z}^2}{f(z)}}}. \quad (3.7)$$

Setting the constant $t_0 = 0$, we impose the initial conditions $\dot{z}(t=0) = 0$ and $z(t=0) = \epsilon$. Here ϵ is a very small number, acting as UV cutoff. These initial conditions imply $\mathcal{H} = \frac{1}{\epsilon}$. Hence the Hamiltonian should be large to allow the initial position of the particle being close to the boundary ($\epsilon \rightarrow 0$). In other words, we start with an excitation (an operator, dual to the massive particle) defined in the UV with large energy \mathcal{H} (large conformal dimension in the UV). This excitation evolves in the QFT. In the dual description, the particle falls in the z -direction following the equation (3.6). First, let us gain some intuition for the motion $z(t)$ using the UV and IR expansions of eq.(3.6). After that, we present an exact analytic solution that confirms the expansions discussed below.

3.1 Asymptotic expansions in the SUSY case ($\mu = 0$)

It is instructive to consider the UV and the IR behaviour of the equation for the trajectory (3.6), using perturbative expansions. This analysis is useful to get an intuitive understanding. After this, we present an exact integration of eq.(3.6). We focus here on the SUSY case $\mu = 0$, which makes the parameters $\bar{\alpha} = \mathcal{H}^2$; $\beta = 0$; $\gamma = Q^6 l^6$; $\zeta = Q^6 l^6 \mathcal{H}^2$. First, consider the expansion of the integrand near $z = \epsilon = 1/\mathcal{H}$,

$$\left. \frac{z}{\sqrt{-1 + \mathcal{H}^2 z^2 + (Ql)^6 z^6 - (Ql)^6 \mathcal{H}^2 z^8}} \right|_{z \sim \frac{1}{\mathcal{H}}} = \frac{\mathcal{H}^{3/2}}{\sqrt{2} \sqrt{\mathcal{H}^6 - (Ql)^6} \sqrt{z - \frac{1}{\mathcal{H}}}} + O(z - \frac{1}{\mathcal{H}})^{1/2}, \quad (3.8)$$

$$\begin{aligned} \frac{1}{\mathcal{H}}(t - t_0) &= \int^z d\tilde{z} \frac{\mathcal{H}^{3/2}}{\sqrt{2} \sqrt{\mathcal{H}^6 - (Ql)^6} \sqrt{\tilde{z} - \frac{1}{\mathcal{H}}}} + O(z - \frac{1}{\mathcal{H}})^{3/2} \\ &= \frac{\mathcal{H}^{3/2} \sqrt{2} \sqrt{z - 1/\mathcal{H}}}{\sqrt{\mathcal{H}^6 - (Ql)^6}} + O(z - \frac{1}{\mathcal{H}})^{3/2}. \end{aligned} \quad (3.9)$$

Solving for $z(t)$ with the choice $t_0 = 0$ we have

$$z(t) = \frac{1}{\mathcal{H}} + \frac{\mathcal{H}^6 - (Ql)^6}{2\mathcal{H}^5} t^2 + \dots \quad (3.10)$$

For $\mathcal{H} = \frac{1}{\epsilon}$ and $Q = 0$ we have,

$$z(t) = \epsilon + \frac{1}{2\epsilon} t^2 + \dots \sim \sqrt{t^2 + \epsilon^2}, \quad (3.11)$$

which matches with the result in equation (11) of the paper [12].

More revealing is the expansion close to the end of the space $z = z_*$. In fact, expanding the integrand close to $z = z_* = \frac{1}{Ql}$, we find

$$\left. \frac{z}{\sqrt{-1 + \mathcal{H}^2 z^2 + (Ql)^6 z^6 - (Ql)^6 \mathcal{H}^2 z^8}} \right|_{z \sim \frac{1}{Ql}} = \frac{1}{\sqrt{6} \sqrt{(Ql)^3 - \mathcal{H}^2 Ql} \sqrt{z - \frac{1}{Ql}}} + O(z - \frac{1}{Ql})^{1/2} \quad (3.12)$$

$$\begin{aligned} \frac{1}{\mathcal{H}}(t_e - t) &= \int^z d\tilde{z} \frac{1}{\sqrt{6} \sqrt{(Ql)^3 - \mathcal{H}^2 Ql} \sqrt{\tilde{z} - \frac{1}{Ql}}} + O(z - \frac{1}{Ql})^{3/2} \\ &= \frac{\sqrt{\frac{2}{3}} \sqrt{z - \frac{1}{Ql}}}{\sqrt{(Ql)^3 - \mathcal{H}^2 Ql}} + O(z - \frac{1}{Ql})^{3/2}. \end{aligned} \quad (3.13)$$

The time to reach the end of the space is denoted by t_e . Solving for $z(t)$ with $z(t_e) = \frac{1}{Ql}$ we have

$$z(t) = \frac{1}{Ql} - \frac{3Ql}{2} \left(1 - \frac{(Ql)^2}{\mathcal{H}^2} \right) (t - t_e)^2 + \dots \quad (3.14)$$

As expected, this result is heavily dependent on the parameter Q and the consequent existence of the end of space at z_* .

Having understood the asymptotic behaviour of $z(t)$, we study now an exact analytic expression for $z(t)$ solving eqs.(3.5)-(3.6).

3.2 Exact solution in the SUSY case ($\mu = 0$)

As above, we consider the case $\mu = 0$. The function $f(z)$ is given by $f(z) = 1 - Q^6 l^6 z^6$. As above we set $\bar{\alpha} = \mathcal{H}^2$, $\beta = 0$, $\gamma = (Ql)^6$, $\zeta = (Ql)^6 \mathcal{H}^2$. We exactly perform the integral in eq.(3.5),

$$\frac{t}{\mathcal{H}} = \int_{1/\mathcal{H}}^z d\tilde{z} \frac{\tilde{z}}{\sqrt{-1 + \mathcal{H}^2 \tilde{z}^2 + (Ql)^6 \tilde{z}^6 - (Ql)^6 \mathcal{H}^2 \tilde{z}^8}} \quad (3.15)$$

$$= \int_{1/\mathcal{H}}^z d\tilde{z} \frac{\tilde{z}}{\sqrt{(\mathcal{H}^2 \tilde{z}^2 - 1)(1 - (Ql)^6 \tilde{z}^6)}}. \quad (3.16)$$

We do a change of variable $u = (Ql)^2 \tilde{z}^2$ and introduce the parameter $\alpha \equiv \mathcal{H}^2 / (Ql)^2$. Now,

$$\frac{t}{\mathcal{H}} = \frac{1}{2(Ql)^2 \sqrt{\alpha}} \int_{1/\alpha}^{(Ql)^2 z^2} du \frac{1}{\sqrt{(u - 1/\alpha)(1 - u)(u^2 + u + 1)}}. \quad (3.17)$$

Eq.(3.17) is in the form of an incomplete elliptic integral of the first kind as explained in Appendix A, in particular in eq.(A.1). We use the terminology and abbreviations for the elliptic functions and integrals defined in Appendix A, specifically in section A.1, where we carefully evaluate the integral in eq.(3.17) and invert to find $z(t)$. The result for $z(t)$ is

$$z(t) = \frac{1}{Ql} \sqrt{\frac{\frac{A}{\alpha} \left(1 + \text{cn}\left(\frac{2Ql}{g}t, k\right)\right) + B \left(1 - \text{cn}\left(\frac{2Ql}{g}t, k\right)\right)}{A \left(1 + \text{cn}\left(\frac{2Ql}{g}t, k\right)\right) + B \left(1 - \text{cn}\left(\frac{2Ql}{g}t, k\right)\right)}}. \quad (3.18)$$

We have defined the following constants,

$$g = \left[\frac{\alpha^2}{3\alpha^2 + 3\alpha + 3} \right]^{\frac{1}{4}}, \quad k^2 = \frac{-3(1 + \alpha) + 2\sqrt{3(\alpha^2 + \alpha + 1)}}{4\sqrt{3(\alpha^2 + \alpha + 1)}}. \quad (3.19)$$

$$A = \sqrt{3}, \quad B = \sqrt{\frac{\alpha^2 + \alpha + 1}{\alpha^2}}.$$

We also denoted by $\text{cn}(x, k)$ the Elliptic cosine function. For definitions, important relations with other Elliptic functions and integrals, see Appendix A.

In Figure 1 we plot $z(t)$ for the values $Ql = [\frac{1}{10}, 1, 2]$ and $\mathcal{H} = 10$. The results can be compared with the case of pure AdS in the lower panel of Figure 1. Note that as Ql decreases, we recover the pure AdS case.

With this analytic solution, we can calculate the time taken to reach the end of the space, imposing that $z(t_e) = \frac{1}{Ql}$. The result is

$$t_e = \left(\frac{g}{Ql} \right) K(k) = \frac{\sqrt{\alpha}}{Ql[3(\alpha^2 + \alpha + 1)]^{\frac{1}{4}}} K \left[\frac{\sqrt{-3(1 + \alpha) + 2\sqrt{3(\alpha^2 + \alpha + 1)}}}{2[3(\alpha^2 + \alpha + 1)]^{\frac{1}{4}}} \right]. \quad (3.20)$$

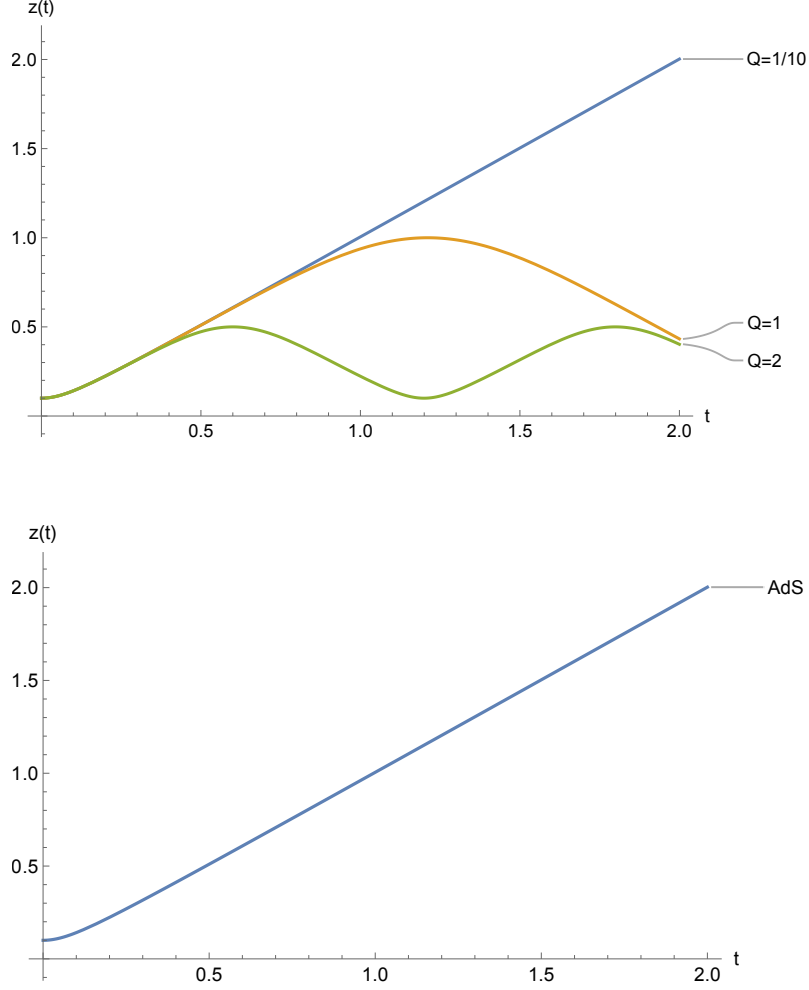


Figure 1. The function $z(t)$ for choices of $(Ql) = 1/10, 1, 2$ and $\mathcal{H} = 10$ (Upper panel) and the function $z(t)$ for pure AdS background ($Q = 0$) (Lower panel).

where $K(x) = \int_0^{\frac{\pi}{2}} \frac{dt}{\sqrt{1-x^2 \sin^2 t}}$ is the elliptic integral of the first kind. We can expand $z(t)$ close to the boundary and the end of space, $z(0) = \frac{1}{\mathcal{H}}$ and $z(t_e) = \frac{1}{Ql}$. We obtain precisely the asymptotic expansions in eqs.(3.10) and (3.14) respectively. Furthermore two consistency checks of our solution in eq.(3.18) are the following: for $\alpha = 1$ (or $\mathcal{H} = Ql$), when the UV-cutoff and the IR-end-of-space do coincide, we find $z = \frac{1}{Ql} = \epsilon$ and $t_e = 0$. On the other hand for $\alpha \rightarrow \infty$ (keeping the UV cutoff large and sending $Ql \rightarrow 0$), we find that $t_e \sim \frac{1}{Ql} \rightarrow \infty$, in agreement for the time taken by a massive particle in AdS to reach the horizon from the boundary.

Considering an expansion of (3.18) in the limit $Ql \rightarrow 0$ and $\alpha \rightarrow \infty$, one finds

$$z(t) = \frac{1}{\sqrt{\alpha}} \frac{1}{Ql} + \frac{\sqrt{\alpha} Ql}{2} t^2 + \dots \quad (3.21)$$

which boils down into an expansion as in pure AdS (3.11) by remembering the fact that $\alpha = \frac{1}{\epsilon^2 Q^2 l^2}$. In other words, this is the limit in which the cigar transits into a pure AdS and

the proper momentum increases indefinitely. All this analysis is in agreement with Figure 1.

Let us now define the momentum that allows us to calculate the complexity.

4 The proper momentum and complexity

Following the observation made in Ref. [12], we need to define a new radial coordinate, which is conjectured to be related to the Krylov basis on the field theory side. We would like to define a *proper radial distance*, such that when in the geodesic distance between two points obtained from the metric in eq. (2.1), conditions such as $\Delta t = 0$, $\Delta x_1 = \Delta x_2 = \Delta \phi = 0$, and similar conditions for internal S^5 directions, are chosen, then, $\Delta s = \Delta \bar{\rho}$ or $ds^2 = d\bar{\rho}^2$. The new radial coordinate measures the proper distance between two points in the space in a fixed time-slice and also fixing other coordinates ($\Delta t = 0$, $\Delta x_1 = 0, \dots$). Hence, we define our new coordinate in terms of the radial coordinate z as

$$ds_{proper}^2 = l^2 \frac{dz^2}{z^2 f(z)} \equiv d\bar{\rho}^2, \quad \Rightarrow \quad -d\bar{\rho} = \frac{ldz}{z\sqrt{f(z)}}. \quad (4.1)$$

The minus sign is chosen as the $\bar{\rho}$ increases while z decreases.

For the particular case that occupies us here, $f(z) = 1 - (Ql z)^6$ we find

$$z = \frac{1}{Ql \left[\cosh \left(\frac{3\bar{\rho}}{l} \right) \right]^{\frac{1}{3}}}. \quad (4.2)$$

Notice that the limit $\bar{\rho} \rightarrow \infty$ implies $z \rightarrow 0$ indicating the UV of the QFT. Also, in this case of large $\bar{\rho}$ we have $z \sim e^{-\frac{\bar{\rho}}{l}}$, in agreement with the change of coordinates that brings us to a Krylov basis as proposed in [12]. In contrast, for $\bar{\rho} \rightarrow 0$ we reach $z_* = \frac{1}{Ql}$.

The rate of change of the complexity is defined in terms of the *proper momentum* $P_{\bar{\rho}}$ as [12],

$$\partial_t \mathcal{C}(t) \propto P_{\bar{\rho}} = P_z \frac{\partial \dot{z}}{\partial \dot{\bar{\rho}}} = -\frac{\dot{z}}{l\sqrt{f(z)}} \frac{1}{\sqrt{1 - \frac{\dot{z}^2}{f(z)}}}. \quad (4.3)$$

The expansions of this quantity close to the boundary and end of space are

$$\partial_t \mathcal{C}(t) \propto P_{\bar{\rho}} \Big|_{t \sim 0} = -\frac{\sqrt{\mathcal{H}^6 - (Ql)^6}}{\mathcal{H}^2 l} t + O(t)^2. \quad (4.4)$$

$$P_{\bar{\rho}} \Big|_{t \sim t_e} = \pm \frac{\sqrt{\mathcal{H}^2 - (Ql)^2}}{Ql^2} + O(t - t_e)^2. \quad (4.5)$$

The UV behaviour, in the limit $Ql \rightarrow 0$, is the same one found in equation (19) of the paper [12]. In contrast, the IR behaviour is significantly altered by the presence of the parameter Q . Notice that in $Ql \rightarrow 0$ limit the end of space is moved to $z \rightarrow \infty$, and the momentum diverges. This agrees with the original analysis in pure AdS with $Ql = 0$, for which the momentum at large times diverges.

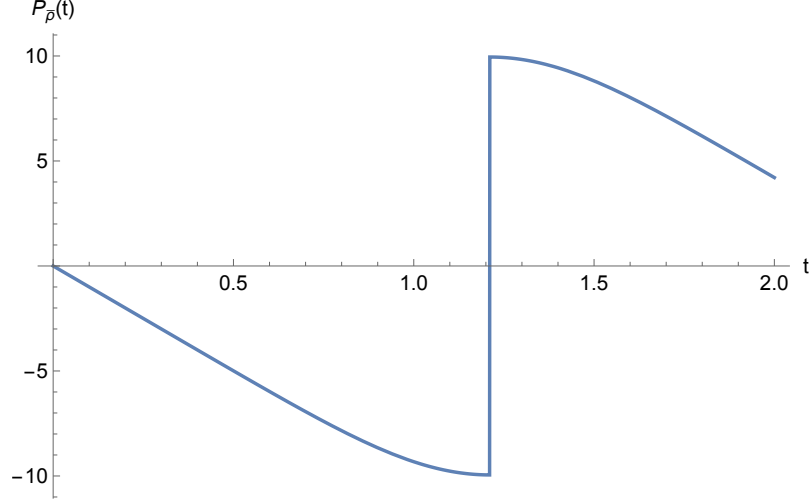


Figure 2. $P_{\bar{\rho}}(t)$ for $Ql = 1$ and $\mathcal{H} = 10$. The particle reaches to the end of space at $t_e \simeq 1.21$.

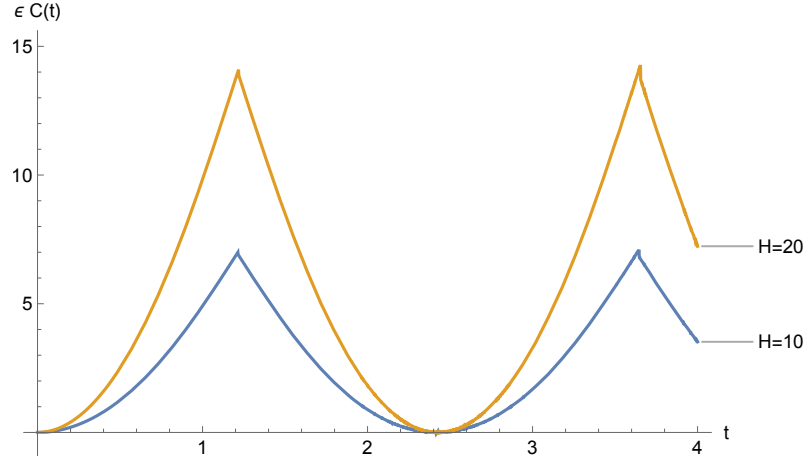


Figure 3. $\epsilon \mathcal{C}(t)$, for $Ql = 1$ and $\mathcal{H} = 10, 20$.

Figure 2 provides a plot for momentum with choices of $Ql = 1$ and $\mathcal{H} = 10$. This matches with the pure AdS case in the $Q \rightarrow 0$ limit. Note that the charge Q has a non-trivial effect on both the UV and IR expansions.

Finally, in Figure 3, a plot for the complexity $\mathcal{C}(t)$, being proportional to the integral of the proper momentum,

$$\mathcal{C}(t) = - \int dt \frac{P_{\bar{\rho}}(t)}{\epsilon}, \quad (4.6)$$

as a function of time for different choices of parameters, is provided. Here ϵ is the proportionality constant which in [12], it is taken to be $\epsilon = 1/\mathcal{H}$ to match with the CFT results. One can adopt the same convention here, but other choices might be possible to match with the QFT calculation which is left for a future work.

Some observations follow. Since the space ends at a finite distance in the radial coordinate, the particle, initially at rest close to the boundary, reaches the end of space in a

finite time. Its proper momentum is finite and changes sign after hitting the end of space at $t = t_e$. Then the particle bounces back, returning to the initial point and the oscillatory motion continues. As a result of this oscillatory motion, the complexity, as depicted in Figure 3, also oscillates. This type of behaviour had been observed before in the literature—see, for instance, [10, 12, 39] for CFT on a finite line or [10, 40] for compact group manifolds. In those cases, the behaviour was attributed to the finiteness of the Hilbert space of the theories under consideration.

The same applies for the case studied here. As discussed in detail in [23, 24], the dual theories are gapped in the IR. The initial condition for the particle, as $z(t = 0) = 1/\mathcal{H}$, sets a UV cutoff in the dual theory, as is also mentioned in [12]. Hence, the Hilbert space available for the dual state or the operator is finite dimensional and the oscillatory behavior for the complexity follows. One can deduce from Figure 3 that the larger \mathcal{H} is, the larger is the maximum value for the complexity (and it is achieved at $t = t_e$). We conjecture that this is the result of an increase in the number of states in the dual Hilbert space.

It is also constructive to mention the interpretation from Ref. [41] in which the falling of particles under influence of gravity is attributed to the tendency of the dual state to get more complex. The second time derivative of the complexity will be proportional to the time derivative of the proper momentum of the particle which can be interpreted as an effective ‘force’. Thus, when the particle moves against the direction of the gravity after hitting the end of space, the dual complexity takes a decreasing form.

We can make contact with the interesting work [18]. In that paper, working with a modified (confining) version of the Ising model, it was proposed that the Krylov complexity could act as an order parameter indicating confinement. It was found that in a modified version of the Ising model, the growth of complexity qualitatively decreases with respect to the (undeformed) Ising model, showing pronounced oscillations. We observe a similar behaviour. In our case for a model for a SCFT₄ that flows to a confining and gapped three-dimensional QFT. It is natural to wonder if the scales at which the oscillations occur in our system (the different times for which the complexity changes slope) are in some way related to mass-scales in the QFT. One might compare this with the scale of glueballs in this system. For papers that computed glueballs in related systems see [20, 33, 35, 42].

4.1 A field theoretical approach?

Let us briefly indicate how to approach the problem of computing the complexity from the point of view of the QFT. As we mentioned, for very large energies our QFT is $\mathcal{N} = 4$ SYM compactified on S^1 , plus a twist with the R-symmetry to preserve four SUSYs. The *perturbative* Lagrangian is written in detail in the papers [30, 32]. The *perturbative* spectrum consists of a massless gauge field and a massless gaugino, plus a tower of bosons and fermions (forming SUSY multiplets), with known (non-zero) masses. For each one of these fields the complexity can be calculated. In fact, papers like [9, 15, 43–46] make field theoretical calculations that, once assembled, could calculate the complexity for a perturbative lagrangian like the one of our system.

The problem with applying the above reasoning to our case is that the spectrum of the field theory dual to the Anabalón-Ross background consists of a tower of massive glueballs

(of spin zero, one and two) and the partner (fermionic) gluebalinos. In rigour, we should aim at a calculation that generalises the one in [15]. Indeed, the authors of [15] consider simple lagrangians like

$$L \sim \sum_{n=1}^{\infty} (\partial\phi_n)^2 - m_n^2 \phi_n^2. \quad (4.7)$$

They use eq.(4.7) to model a theory with a mass gap and a known discrete spectrum. With this Lagrangian and compactifying the space time, they compute a two point correlator $\langle e^{-\beta H/2} \phi_n(t, x) e^{-\beta H/2} \phi_n(0, x) \rangle$. Using this correlator one can compute the wavefunction $\psi_n(t)$ satisfying the Krylov condition and from there determine the Krylov complexity $K(t) = \sum_{n=1}^{\infty} n |\psi_n(t)|^2$.

The problem is that the field theory dual to our background is more elaborated. As we anticipated, it contains composites of spin $S = 0, 1, 2$ (with fermionic partners of spin $S = \frac{1}{2}, \frac{3}{2}$). The full mass spectrum is not known at present, but can be computed as we indicate below.

One can do a simple computation for the spin-two glueballs, along the lines of those done for related systems in [20, 33, 35]. One may also attempt to get the mass spectrum of a probe scalar as done in [42]. But what we really need is a more dedicated job: in five dimensional AdS-supergravity consistently fluctuate the metric, gauge fields and scalars, keep to second order in the fluctuations, identify the gauge invariant combination of fluctuations, diagonalise the system of ODE and calculate the spectrum of masses. This calculation was done (for a related system) in [47]. It would be interesting to repeat such computation in the five-dimensional $U(1)$ gauged supergravity whose lift to IIB gives the Anabalón-Ross background.

As this calculation is not done in the bibliography, at this time, we need to conform ourselves with a qualitative agreement: in [15] for systems with a non-conformal UV or in [18] for a system on the lattice, the authors find that confining systems display oscillations in the complexity, as we have found in our well defined set-up. Let us close this paper with some summary and conclusions.

5 Conclusions and Outlook

Let us start with an ‘executive summary’ of the contents of this work: *we have presented the holographic dual to a properly defined confining QFT (with a UV conformal point and a gapped IR). We analytically computed the Krylov complexity using this holographic dual. We obtained an oscillatory behaviour consistent with the one found in lattice systems [14, 18]. Other numerical holographic results [15] qualitatively agree with our analytic findings.*

A more detailed summary goes as follows: Section 1 motivates the study of holographic Krylov (spread) complexity in confining gauge theories, extending recent proposals that identify the time derivative of Krylov complexity with the proper radial momentum of a bulk particle [12]. We argue that confining geometries, unlike AdS spaces, generate a natural finite Hilbert-space truncation through the presence of both a UV cutoff and an IR end-of-space. This motivates analysing complexity in a fully top-down setting.

Section 2 reviews the Anabalón–Ross solitonic background—an analytic Type IIB solution that implements a twisted-circle compactification of $\mathcal{N} = 4$ SYM that flows to a 3d confining, gapped theory. We also lay out the geometric parameters (Q, μ) that control the IR endpoint and supersymmetry.

In Section 3, we study geodesic motion of a probe particle in this background. We first obtain UV and IR asymptotic expansions, showing that while UV behaviour reproduces the standard AdS result, the IR structure is qualitatively modified by the finite endpoint at $z = z_*$. We then derive an exact analytic solution for the trajectory $z(t)$ in terms of Jacobi elliptic functions, allowing the precise calculation of the time needed for the probe to reach the end of space. Section 4 uses this solution to compute the proper radial momentum and thus the Krylov complexity, finding that both become oscillatory due to reflections at the IR wall—an effect interpreted as an holographic signature of the finite Hilbert space of the dual QFT. The section also discusses how these features compare to expectations from QFT and to related studies of complexity in confining systems. We briefly comment on the field theory computation that one should do, to calculate the complexity using the QFT-description of our system.

The Appendices A and B discuss in great detail the Elliptic integrals found in this paper either for the SUSY case or for a geodesic in a generic Anabalón–Ross background.

The exact (analytic) results of this paper motivates various avenues for future work. Let us list some points that would be nice to address in future work.

- It would be interesting to explicitly perform the calculation advanced in Section 4.1. This is to compute Lanczos coefficients and spread complexity directly in the twisted-circle compactification of $\mathcal{N}=4$ SYM, dual to the Anabalón–Ross background.
- Extend to nonzero angular momentum and operator quantum numbers: study geodesics and probes charged under the internal isometries — these correspond to operators with R-charge and could reveal richer operator growth patterns (e.g., mixing, multi-mode behaviour).
- Study SUSY vs SUSY-broken flows: perform a systematic comparison of the case $\mu = 0$ (preserves four supercharges) against the $\mu > 0$ case. This can quantify how supersymmetry affects complexity saturation, oscillation amplitude, etc.
- Compare different complexity notions: given other holographic complexity diagnostics (for example, complexity-equals-volume or complexity-equal-area, subregion complexity) in the same background (see for example [20, 25, 37]) and compare qualitative/quantitative features with Krylov/spread complexity. This might help decide which features are universal signatures of confinement.
- It would be nice (but hard!) to go beyond probe particle approximation by including backreaction of the heavy excitation.
- It is interesting to study string/brane probes, to learn about complexity for classes of operator whose dynamics cannot be captured by point particles.

- It could be feasible to numerically explore the space of parameters in the model. This is to map the dependence of observable quantities like t_e , oscillation amplitudes and complexity maxima over the (Q, μ, H) parameter space and compare with the glueball spectrum of the Anabalón-Ross model. This could make quantitative the statement that geometric IR scales control complexity features.
- It may be feasible to investigate the connection to chaos bounds and operator growth. In more detail, to examine whether the early time growth of Krylov complexity (or Lanczos coefficients) in this holographic model respects the conjectured bounds on operator growth.
- It would be interesting to repeat our calculation in variations of the Anabalón-Ross model, like the works [20, 23–25, 29], etc.
- It would be really very nice to be able to test our qualitative conclusions (oscillations, saturation) against lattice simulations of compactified gauge theories or tensor-network toy models that implement a gapped spectrum. This would increase confidence that the bulk-derived signals are true field theory effects.

We hope to report on some of these points in the near future.

Acknowledgments

For discussions, for comments on the manuscript, and for sharing their ideas with us, we wish to thank: Dmitry Ageev, Nicolás Bragagnolo, Alfonso Ramallo, Ricardo Terrazas. The work of HN is supported in part by CNPq grant 304583/2023-5 and FAPESP grant 2019/21281-4. HN would also like to thank the ICTP-SAIFR for their support through FAPESP grant 2021/14335-0. DR would like to acknowledge the Mathematical Research Impact Centric Support (MATRICS) grant (MTR/2023/000005) received from ANRF, India

Open Access Statement — For the purpose of open access, the authors have applied a Creative Commons Attribution (CC BY) license to any Author Accepted Manuscript version arising.

A Elliptic Integrals

In this appendix, we present the prescription to calculate certain integrals appearing in the body of the paper. They will be used extensively to calculate different observables.

We will introduce terminology and abbreviations for the elliptic functions and integrals which are required to perform our calculations, following [48].

For the integral of the form

$$\int_b^y \frac{du}{\sqrt{(a-u)(u-b)(u-c)(u-\bar{c})}}, \quad (\text{A.1})$$

with a, b real, $a \geq y > b, c, \bar{c}$ complex, which is in the form of an incomplete elliptic integral of the first kind. One finds

$$\begin{aligned} \sqrt{(a-u)(u-b)(u-c)(u-\bar{c})} &= \sqrt{(a-u)(u-b) \left[(u-b_1)^2 + a_1^2 \right]}; \\ b_1 &= \frac{c + \bar{c}}{2}, \quad a_1^2 = -\frac{(c - \bar{c})^2}{4}. \end{aligned} \quad (\text{A.2})$$

Now one can define a change of variable from u to \bar{u} with the following relations

$$\begin{aligned} \mathbf{cn}(\bar{u}, k) &= \frac{(a-u)B - (u-b)A}{(a-u)B + (u-b)A}, \quad A^2 = (a-b_1)^2 + a_1^2, \\ B^2 &= (b-b_1)^2 + a_1^2, \quad g = \frac{1}{\sqrt{AB}}, \quad k^2 = \frac{(a-b)^2 - (A-B)^2}{4AB}. \end{aligned} \quad (\text{A.3})$$

Here, ‘ \mathbf{cn} ’ is the elliptic cosine function. The upper limit of the integral in eq.(A.1), y , gets mapped to a new parameter that we would like to call it u_1 . Later, it turns out to be convenient to have φ defined below in terms of the u_1 variable or originally y ,

$$\mathbf{cn}(u_1, k) = \cos \varphi, \quad \varphi = \text{am}(u_1, k) = \cos^{-1} \left[\frac{(a-y)B - (y-b)A}{(a-y)B + (y-b)A} \right], \quad (\text{A.4})$$

where ‘ am ’, is the Jacobi amplitude defined here as $\text{am}(x, k) \equiv \cos^{-1} \mathbf{cn}(x, k)$.

Then the integral in eq.(A.1) takes the following form,

$$\begin{aligned} \int_b^y \frac{du}{\sqrt{(a-u)(u-b)(u-c)(u-\bar{c})}} &= g \int_0^{u_1} d\bar{u} = g u_1 = g \mathbf{cn}^{-1}(\cos \varphi, k) \\ &= g \mathbf{F}(\varphi, k). \end{aligned} \quad (\text{A.5})$$

The definition of ‘ am ’ and ‘ \mathbf{cn} ’ functions are implicitly given among the above relations. Here, ‘ \mathbf{F} ’ is the incomplete elliptic integral of the first kind defined below,

$$\int_0^\varphi \frac{d\theta}{\sqrt{1 - k^2 \sin^2 \theta}} \equiv \mathbf{F}(\varphi, k). \quad (\text{A.6})$$

Note the appearance of k^2 in the denominator of the integral, but k in the argument of the \mathbf{F} function, as different conventions are employed in the literature. Specially, Mathematica software’s definition requires k^2 as the second argument of the ‘ \mathbf{F} ’ function to match our definition which has only k appearing as the second argument.

A.1 An explicit calculation

In this section we give a detailed derivation of the result for the $z(t)$ function presented in eq.(3.18) in the body of the paper.

The integral

$$\frac{t}{\mathcal{H}} = \frac{1}{2(Ql)^2 \sqrt{\alpha}} \int_{1/\alpha}^{(Ql)^2 z^2} du \frac{1}{\sqrt{(u - 1/\alpha)(1-u)(u^2 + u + 1)}}, \quad (\text{A.7})$$

also given in eq.(3.17), is in the form of an incomplete elliptic integral of the first kind as explained above.

Now we define the new parameters given in eqs. (A.2-A.4) required in the final integral result as

$$\begin{aligned}
a &= 1, \quad b = 1/\alpha, \quad c = e^{2\pi i/3}, \quad \bar{c} = e^{-2\pi i/3}; \quad b_1 = -1/2, \quad a_1^2 = 3/4, \\
A^2 &= 3, \quad B^2 = \frac{\alpha^2 + \alpha + 1}{\alpha^2}, \quad g = \left[\frac{\alpha^2}{3\alpha^2 + 3\alpha + 3} \right]^{\frac{1}{4}}, \\
k^2 &= \frac{-3(1 + \alpha) + 2\sqrt{3(\alpha^2 + \alpha + 1)}}{4\sqrt{3(\alpha^2 + \alpha + 1)}}, \\
\varphi &= \text{am}(u_1, k) = \cos^{-1} \left[\frac{(1 - (Ql)^2 z^2)B - ((Ql)^2 z^2 - 1/\alpha)A}{(1 - (Ql)^2 z^2)B + ((Ql)^2 z^2 - 1/\alpha)A} \right]. \tag{A.8}
\end{aligned}$$

Here, ‘am’ is the Jacobi amplitude defined in the previous section. The variables φ and u_1 are given implicitly in terms of z in the last relation of the eq.(A.8).

Then, using eq. (A.5), one finds

$$\begin{aligned}
\frac{t}{\mathcal{H}} &= \frac{1}{2(Ql)^2 \sqrt{\alpha}} \int_{1/\alpha}^{(Ql)^2 z^2} du \frac{1}{\sqrt{(u - 1/\alpha)(1 - u)(u^2 + u + 1)}} = \frac{g}{2(Ql)^2 \sqrt{\alpha}} u_1 \tag{A.9} \\
&= \frac{g}{2(Ql)^2 \sqrt{\alpha}} \mathbf{F}(\varphi, k).
\end{aligned}$$

We insert φ and k from eq.(A.8) and obtain

$$\frac{t}{\mathcal{H}} = \frac{g}{2(Ql)^2 \sqrt{\alpha}} \mathbf{F}(\cos^{-1} \left[\frac{(1 - (Ql)^2 z^2)B - ((Ql)^2 z^2 - 1/\alpha)A}{(1 - (Ql)^2 z^2)B + ((Ql)^2 z^2 - 1/\alpha)A} \right], \sqrt{\frac{(1 - 1/\alpha)^2 - (A - B)^2}{4AB}}), \tag{A.10}$$

‘ \mathbf{F} ’ being the incomplete elliptic integral of the first kind defined in eq.(A.6). Using the relations among elliptic integrals and Jacobi functions one can invert the above relations and solve for $z(t)$. One has

$$\begin{aligned}
\varphi &= \text{am}(u_1, k) \rightarrow \mathbf{cn}(u_1, k) \equiv \cos \text{am}(u_1, k) = \cos \varphi = \frac{(1 - (Ql)^2 z^2)B - ((Ql)^2 z^2 - 1/\alpha)A}{(1 - (Ql)^2 z^2)B + ((Ql)^2 z^2 - 1/\alpha)A} \\
z(t) &= \frac{1}{Ql} \sqrt{\frac{\frac{A}{\alpha}(1 + \mathbf{cn}(u_1, k)) + B(1 - \mathbf{cn}(u_1, k))}{A(1 + \mathbf{cn}(u_1, k)) + B(1 - \mathbf{cn}(u_1, k))}}. \tag{A.11}
\end{aligned}$$

Recalling $u_1 = \frac{2(Ql)}{g}t$ from eq.(A.9), we get

$$z(t) = \frac{1}{(Ql)} \sqrt{\frac{A/\alpha(1 + \mathbf{cn}(\frac{2(Ql)}{g}t, k)) + B(1 - \mathbf{cn}(\frac{2(Ql)}{g}t, k))}{A(1 + \mathbf{cn}(\frac{2(Ql)}{g}t, k)) + B(1 - \mathbf{cn}(\frac{2(Ql)}{g}t, k))}}, \tag{A.12}$$

which is the desired final result given in the body of the paper.

B Exact solution for $\mu \neq 0$ and $Q \neq 0$

In this section, we consider the generic case $\mu \neq 0, Q \neq 0$, where the function $f(z)$ is given by $f(z) = 1 - \mu l^2 z^4 - Q^6 l^6 z^6$. Furthermore, we set $\bar{\alpha} = \mathcal{H}^2$, $\beta = \mu l^2$, $\gamma = Q^6 l^6 - \mu \mathcal{H}^2 l^2$, $\zeta = Q^6 l^6 \mathcal{H}^2$.

Here we perform the integral in eq.(3.5), exactly. We have

$$\frac{t}{\mathcal{H}} = \int_{1/\mathcal{H}}^z d\tilde{z} \frac{\tilde{z}}{\sqrt{f(\tilde{z})(\mathcal{H}^2 \tilde{z}^2 - 1)}} \quad (\text{B.1})$$

$$= \int_{1/\mathcal{H}}^z d\tilde{z} \frac{\tilde{z}}{\sqrt{(\mathcal{H}^2 \tilde{z}^2 - 1)(1 - \mu l^2 \tilde{z}^4 - (Ql)^6 \tilde{z}^6)}}. \quad (\text{B.2})$$

We do a change of variable $u = (Ql)^2 \tilde{z}^2$ and introduce the parameter $\alpha \equiv \mathcal{H}^2 / (Ql)^2$. Now,

$$\frac{t}{\mathcal{H}} = \frac{1}{2(Ql)^2 \sqrt{\alpha}} \int_{1/\alpha}^{(Ql)^2 z^2} du \frac{1}{\sqrt{(u - 1/\alpha)(-u^3 - \frac{\mu}{Q^4 l^2} u + 1)}}. \quad (\text{B.3})$$

Eq.(B.3) is in the form of an incomplete elliptic integral of the first kind. Now, we use the same relations as the ones in the previous Appendix A.

We need to find the roots of the cubic function $-u^3 - \frac{\mu}{Q^4 l^2} u^2 + 1 \equiv (a - u)(u - c)(u - \bar{c})$ appearing in the denominator. The roots are calculable analytically; here we mention the real root denoted as a , related to the position of the end of space, and b_1 and a_1 related to the sum and difference of complex roots.

$$\begin{aligned} a &= \frac{\sqrt[3]{-\frac{2\mu^3}{Q^{12}l^6} - 3\sqrt{81 - \frac{12\mu^3}{Q^{12}l^6} + 27}} + \sqrt[3]{3\left(\sqrt{81 - \frac{12\mu^3}{Q^{12}l^6} + 9}\right) - \frac{2\mu^3}{Q^{12}l^6}}}{3\sqrt[3]{2}} - \frac{\mu}{3Q^4 l^2} \\ b_1 &= \frac{c + \bar{c}}{2} = -\frac{\sqrt[3]{-\frac{2\mu^3}{Q^{12}l^6} - 3\sqrt{81 - \frac{12\mu^3}{Q^{12}l^6} + 27}} + \sqrt[3]{3\left(\sqrt{81 - \frac{12\mu^3}{Q^{12}l^6} + 9}\right) - \frac{2\mu^3}{Q^{12}l^6}}}{6\sqrt[3]{2}} - \frac{\mu}{3Q^4 l^2}, \\ a_1^2 &= -\frac{(c - \bar{c})^2}{4} = \frac{\left(\sqrt[3]{-\frac{2\mu^3}{Q^{12}l^6} - 3\sqrt{81 - \frac{12\mu^3}{Q^{12}l^6} + 27}} - \sqrt[3]{3\left(\sqrt{81 - \frac{12\mu^3}{Q^{12}l^6} + 9}\right) - \frac{2\mu^3}{Q^{12}l^6}}\right)^2}{12 * 2^{2/3}}. \end{aligned} \quad (\text{B.4})$$

These relations reduce to the relevant equations in section A.1 in the $\mu \rightarrow 0$ limit. Now, one can define the required parameters, which are kept implicit for the peace of mind of the reader.

$$\begin{aligned} A^2 &= (a - b_1)^2 + a_1^2, \quad B^2 = (b - b_1)^2 + a_1^2, \quad g = \frac{1}{\sqrt{AB}}, \quad k^2 = \frac{(a - b)^2 - (A - B)^2}{4AB}, \\ b &= 1/\alpha, \quad \text{cn } u_1 = \cos \varphi, \quad \varphi = \text{am } u_1 = \cos^{-1} \left[\frac{(a - (Ql)^2 z^2)B - ((Ql)^2 z^2 - b)A}{(a - (Ql)^2 z^2)B + ((Ql)^2 z^2 - b)A} \right]. \end{aligned} \quad (\text{B.5})$$

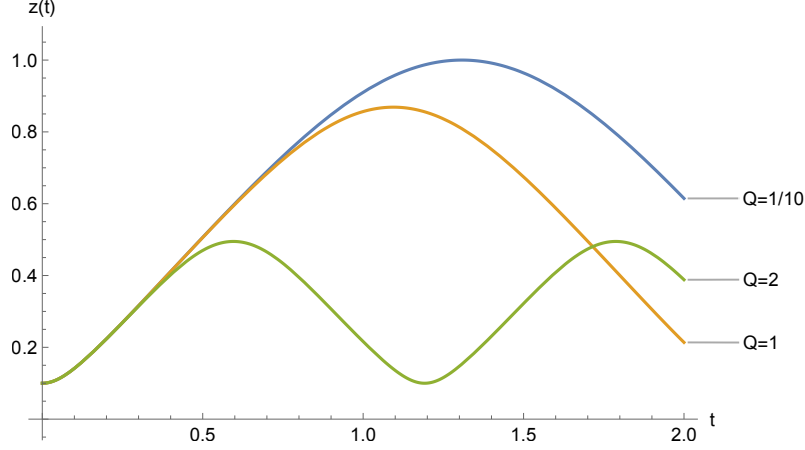


Figure 4. $z(t)$ for various values of Q and $\mu = 1$.

Then,

$$\begin{aligned}
\frac{t}{\mathcal{H}} &= \frac{1}{2(Ql)^2\sqrt{\alpha}} \int_{1/\alpha}^{(Ql)^2 z^2} du \frac{1}{\sqrt{(u - 1/\alpha)(a - u)(u - c)(u - \bar{c})}} = \frac{g}{2(Ql)^2\sqrt{\alpha}} u_1 \\
&= \frac{g}{2(Ql)^2\sqrt{\alpha}} \mathbf{cn}^{-1}(\cos \varphi, k) = \frac{g}{2(Ql)^2\sqrt{\alpha}} \mathbf{F}(\varphi, k) \\
&= \frac{g}{2(Ql)^2\sqrt{\alpha}} \mathbf{F}(\cos^{-1} \left[\frac{(a - (Ql)^2 z^2)B - ((Ql)^2 z^2 - 1/\alpha)A}{(a - (Ql)^2 z^2)B + ((Ql)^2 z^2 - 1/\alpha)A} \right], \sqrt{\frac{(a - 1/\alpha)^2 - (A - B)^2}{4AB}})
\end{aligned} \tag{B.6}$$

Using the relations among elliptic integrals and Jacobi functions, one can invert the above relations and solve for $z(t)$. One has

$$\begin{aligned}
\varphi &= \text{am}(u_1, k) \rightarrow \mathbf{cn}(u_1, k) \equiv \cos \text{am}(u_1, k) = \frac{(a - (Ql)^2 z^2)B - ((Ql)^2 z^2 - 1/\alpha)A}{(a - (Ql)^2 z^2)B + ((Ql)^2 z^2 - 1/\alpha)A} \\
z(t) &= 1/(Ql) \sqrt{\frac{A/\alpha(1 + \mathbf{cn}(u_1, k)) + aB(1 - \mathbf{cn}(u_1, k))}{A(1 + \mathbf{cn}(u_1, k)) + B(1 - \mathbf{cn}(u_1, k))}}.
\end{aligned} \tag{B.7}$$

Remembering $u_1 = \frac{2(Ql)}{g}t$ from eq.(B.6), we get

$$z(t) = \frac{1}{(Ql)} \sqrt{\frac{A/\alpha(1 + \mathbf{cn}(\frac{2(Ql)}{g}t, k)) + aB(1 - \mathbf{cn}(\frac{2(Ql)}{g}t, k))}{A(1 + \mathbf{cn}(\frac{2(Ql)}{g}t, k)) + B(1 - \mathbf{cn}(\frac{2(Ql)}{g}t, k))}}. \tag{B.8}$$

This is the desired result and we plot $z(t)$ for $Q = 1/10, 1, 2$ and $l = 1, \mu = 1, \mathcal{H} = 10$ in Figure 4.

We can expand $z(t)$ close to boundary and end of space, $z(0) = 1/\mathcal{H}$ and $z(t_e) = \sqrt{a}/(Ql)$, where

$$t_e = \frac{gK(k)}{(Ql)}, \tag{B.9}$$

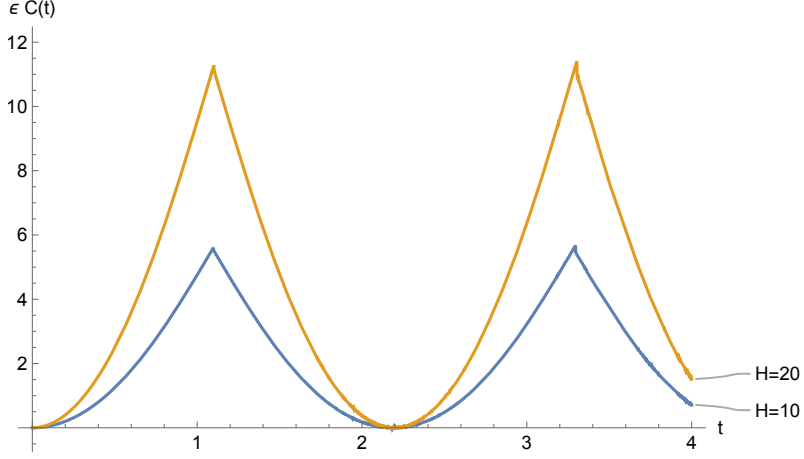


Figure 5. $\epsilon \mathcal{C}(t)$, for $Q = 1, \mu = 1$ and $l = 1$ and $\mathcal{H} = 10, 20$.

with K being the elliptic integral of the first kind.

One gets

$$z(t) \Big|_{t \sim 0} = \frac{1}{\mathcal{H}} + \frac{(Ql)(a-b)(a_1^2 + (b-b_1)^2)}{2\sqrt{b}} t^2 + O(t)^3 = \frac{1}{\mathcal{H}} + \frac{(Ql)f(\frac{\sqrt{b}}{(Ql)})}{2\sqrt{b}} t^2 + O(t)^3, \quad (\text{B.10})$$

$$z(t) \Big|_{t \sim t_e} = \frac{\sqrt{a}}{(Ql)} - \frac{(Ql)(a-b)(a^2 - 2ab_1 + a_1^2 + b_1^2)}{2\sqrt{a}} (t - t_e)^2 + O(t - t_e)^3, \quad (\text{B.11})$$

$$(\text{B.12})$$

matching exactly with eq. (3.10) and eq. (3.14) in the $\mu \rightarrow 0$ limit.

The expansion of the proper momentum in the $\bar{\rho}$ coordinate,

$$-d\bar{\rho} = \frac{ldz}{z\sqrt{f(z)}}, \quad (\text{B.13})$$

close to the boundary and end of the space is

$$\partial_t \mathcal{C}(t) \propto P_{\bar{\rho}} \Big|_{t \sim 0} = -\frac{\sqrt{a-b}\sqrt{a_1^2 + (b-b_1)^2}(Ql)}{\sqrt{b}} t + O(t)^2 = -\frac{\sqrt{f(\sqrt{b}/(Ql))}}{\sqrt{b}/(Ql)} t + O(t)^2. \quad (\text{B.14})$$

$$P_{\bar{\rho}} \Big|_{t \sim t_e} = \pm \frac{\sqrt{a-b}}{\sqrt{b}} + O(t - t_e)^2. \quad (\text{B.15})$$

Remembering $\sqrt{b}/(Ql) = 1/\mathcal{H}$, this matches with the previous results for $\mu \rightarrow 0$ as provided in the previous sections.

A plot for the complexity for $Q = 1, \mu = 1$ and $\mathcal{H} = 10, 20$ is provided in Figure 5.

References

- [1] P. Caputa, J. M. Magan and D. Patramanis, *Geometry of Krylov complexity*, *Phys. Rev. Res.* **4** (2022) 013041 [[2109.03824](#)].
- [2] Z.-Y. Fan, *Momentum-Krylov complexity correspondence*, [2411.04492](#).
- [3] Z.-Y. Fan, *Generalised Krylov complexity*, [2306.16118](#).
- [4] P.-Z. He, *Revisit the relationship between spread complexity rate and radial momentum*, [2411.19172](#).
- [5] E. Rabinovici, A. Sánchez-Garrido, R. Shir and J. Sonner, *A bulk manifestation of Krylov complexity*, *JHEP* **08** (2023) 213 [[2305.04355](#)].
- [6] M. P. Heller, J. Papalini and T. Schuhmann, *Krylov Spread Complexity as Holographic Complexity beyond Jackiw-Teitelboim Gravity*, *Phys. Rev. Lett.* **135** (2025) 151602 [[2412.17785](#)].
- [7] M. P. Heller, F. Ori, J. Papalini, T. Schuhmann and M.-T. Wang, *De Sitter holographic complexity from Krylov complexity in DSSYK*, [2510.13986](#).
- [8] Y. Fu, H.-S. Jeong, K.-Y. Kim and J. F. Pedraza, *Toward Krylov-based holography in double-scaled SYK*, [2510.22658](#).
- [9] P. Nandy, A. S. Matsoukas-Roubeas, P. Martínez-Azcona, A. Dymarsky and A. del Campo, *Quantum dynamics in Krylov space: Methods and applications*, *Phys. Rept.* **1125-1128** (2025) 1 [[2405.09628](#)].
- [10] S. Baiguera, V. Balasubramanian, P. Caputa, S. Chapman, J. Haferkamp, M. P. Heller et al., *Quantum complexity in gravity, quantum field theory, and quantum information science*, [2503.10753](#).
- [11] E. Rabinovici, A. Sánchez-Garrido, R. Shir and J. Sonner, *Krylov Complexity*, [2507.06286](#).
- [12] P. Caputa, B. Chen, R. W. McDonald, J. Simón and B. Strittmatter, *Spread Complexity Rate as Proper Momentum*, [2410.23334](#).
- [13] J. M. Maldacena, *The Large N limit of superconformal field theories and supergravity*, *Adv. Theor. Math. Phys.* **2** (1998) 231 [[hep-th/9711200](#)].
- [14] M. Kormos, M. Collura, G. Takács and P. Calabrese, *Real-time confinement following a quantum quench to a non-integrable model*, *Nature Physics* **13** (2016) 246–249.
- [15] T. Anegawa, N. Iizuka and M. Nishida, *Krylov complexity as an order parameter for deconfinement phase transitions at large N* , *JHEP* **04** (2024) 119 [[2401.04383](#)].
- [16] I. R. Klebanov, D. Kutasov and A. Murugan, *Entanglement as a probe of confinement*, *Nucl. Phys. B* **796** (2008) 274 [[0709.2140](#)].
- [17] U. Kol, C. Nunez, D. Schofield, J. Sonnenschein and M. Warschawski, *Confinement, phase transitions and non-locality in the entanglement entropy*, *Journal of High Energy Physics* **2014** (2014) .
- [18] X. Jiang, J. C. Halimeh and N. S. Srivatsa, *Krylov Complexity Meets Confinement*, [2511.03783](#).
- [19] A. Fatemiabhari, H. Nastase and D. Roychowdhury, *Holographic Krylov complexity in $\mathcal{N} = 4$ SYM*, [2511.19286](#).

- [20] A. Fatemiabhari and C. Nunez, *From conformal to confining field theories using holography*, *JHEP* **03** (2024) 160 [[2401.04158](#)].
- [21] J. Yang and A. R. Frey, *Complexity, scaling, and a phase transition*, *JHEP* **09** (2023) 029 [[2307.08229](#)].
- [22] A. R. Frey, M. P. Grehan and P. Singh, *Holographic complexity of the Klebanov-Strassler background*, [2311.18804](#).
- [23] D. Chatzis, A. Fatemiabhari, C. Nunez and P. Weck, *Conformal to confining SQFTs from holography*, [2405.05563](#).
- [24] D. Chatzis, A. Fatemiabhari, C. Nunez and P. Weck, *SCFT deformations via uplifted solitons*, [2406.01685](#).
- [25] D. Chatzis, M. Hammond, G. Itsios, C. Nunez and D. Zoakos, *Universal Observables, SUSY RG-Flows and Holography*, [2506.10062](#).
- [26] G. T. Horowitz and R. C. Myers, *The AdS / CFT correspondence and a new positive energy conjecture for general relativity*, *Phys. Rev. D* **59** (1998) 026005 [[hep-th/9808079](#)].
- [27] A. Anabalón and S. F. Ross, *Supersymmetric solitons and a degeneracy of solutions in AdS/CFT*, *JHEP* **07** (2021) 015 [[2104.14572](#)].
- [28] A. Anabalón, A. Gallerati, S. Ross and M. Trigiante, *Supersymmetric solitons in gauged $\mathcal{N} = 8$ supergravity*, *JHEP* **02** (2023) 055 [[2210.06319](#)].
- [29] A. Anabalón, H. Nastase and M. Oyarzo, *Supersymmetric AdS Solitons and the interconnection of different vacua of $\mathcal{N} = 4$ Super Yang-Mills*, [2402.18482](#).
- [30] F. Castellani and C. Nunez, *Holography for Confined and Deformed Theories: TsT-Generated Solutions in type IIB Supergravity*, [2410.00094](#).
- [31] M. Giliaberti, A. Fatemiabhari and C. Nunez, *Confinement and screening via holographic Wilson loops*, *JHEP* **11** (2024) 068 [[2409.04539](#)].
- [32] S. P. Kumar and R. Stuardo, *Twisted circle compactification of $\mathcal{N} = 4$ SYM and its Holographic Dual*, [2405.03739](#).
- [33] C. Nunez, M. Oyarzo and R. Stuardo, *Confinement and D5-branes*, *JHEP* **03** (2024) 080 [[2311.17998](#)].
- [34] M. Barbosa, H. Nastase, C. Nunez and R. Stuardo, *Penrose limits of I-branes, twist-compactified D5-branes, and spin chains*, *Phys. Rev. D* **110** (2024) 046015 [[2405.08767](#)].
- [35] C. Nunez, M. Oyarzo and R. Stuardo, *Confinement in $(1 + 1)$ dimensions: a holographic perspective from I-branes*, *JHEP* **09** (2023) 201 [[2307.04783](#)].
- [36] N. Macpherson, P. Merrikin, C. Nunez and R. Stuardo, *Twisted-Circle Compactifications of SQCD-like Theories and Holography*, [2506.15778](#).
- [37] D. Chatzis, M. Hammond, G. Itsios, C. Nunez and D. Zoakos, *Supersymmetric AdS Solitons, Coulomb Branch Flows and Twisted Compactifications*, [2511.18128](#).
- [38] D. Cassani and Z. Komargodski, *EFT and the SUSY Index on the 2nd Sheet*, *SciPost Phys.* **11** (2021) 004 [[2104.01464](#)].
- [39] D. S. Ageev and I. Y. Aref'eva, *When things stop falling, chaos is suppressed*, *JHEP* **01** (2019) 100 [[1806.05574](#)].

- [40] V. Balasubramanian, N. Jokela, A. Pönni and A. V. Ramallo, *Information flows in strongly coupled ABJM theory*, *JHEP* **01** (2019) 232 [[1811.09500](#)].
- [41] L. Susskind, *Complexity and Newton's Laws*, *Front. in Phys.* **8** (2020) 262 [[1904.12819](#)].
- [42] A. Anabalón and H. Nastase, *Universal IR holography, scalar fluctuations, and glueball spectra*, *Phys. Rev. D* **109** (2024) 066011 [[2310.07823](#)].
- [43] R. Jefferson and R. C. Myers, *Circuit complexity in quantum field theory*, *JHEP* **10** (2017) 107 [[1707.08570](#)].
- [44] A. Bhattacharyya, A. Shekar and A. Sinha, *Circuit complexity in interacting QFTs and RG flows*, *JHEP* **10** (2018) 140 [[1808.03105](#)].
- [45] A. Moghimejad and S. Parvizi, *Circuit complexity in $U(1)$ gauge theory*, *Mod. Phys. Lett. A* **36** (2021) 2150240 [[2108.08208](#)].
- [46] A. Avdoshkin, A. Dymarsky and M. Smolkin, *Krylov complexity in quantum field theory, and beyond*, *JHEP* **06** (2024) 066 [[2212.14429](#)].
- [47] A. Fatemiabhari, C. Nunez, M. Piai and J. Rucinski, *On the stability of holographic confinement with magnetic fluxes*, [2411.16854](#).
- [48] P. F. Byrd and M. D. Friedman, *Handbook of Elliptic Integrals for Engineers and Scientists*, vol. 67 of *Grundlehren der mathematischen Wissenschaften*. Springer, 1971, [10.1007/978-3-642-65138-0](#).